

## Unfolding the Dynamics of Suprathermal Electrons: Experimental and Numerical Tools on the TCV Tokamak

S. Coda, S. Alberti, P. Blanchard, T.P. Goodman, M.A. Henderson, P. Nikkola,  
Y. Peysson<sup>a</sup>, O. Sauter

*Centre de Recherches en Physique des Plasmas  
Association EURATOM-Confédération Suisse  
Ecole Polytechnique Fédérale de Lausanne, CH-1015 Lausanne, Switzerland*

*<sup>a</sup>Département de Recherches sur la Fusion Contrôlée, Association EURATOM-CEA,  
CEA/Cadarache, 13108 Saint Paul-lez-Durance Cédex, France*

### 1. Introduction

Non-equilibrium systems are common in nature, and it is therefore not surprising that electron velocity distribution functions in plasmas often depart from the equilibrium Maxwellian state. Accretion disks around neutron stars, solar flares, coronal mass ejections and interplanetary shocks are familiar examples of space plasma settings in which significant suprathermal electron populations are found. The principal means by which we observe and study these electrons, and indeed we know they exist at all, are the radiation fields they emit upon being accelerated either by a magnetic field (cyclotron emission) or by Coulomb collisions, mainly with ions (bremsstrahlung). By studying the properties of the radiation, we seek to understand the fundamental processes that govern the suprathermal distributions: acceleration, momentum and energy transfer to slower particles, spatial diffusion. Additionally, owing to the complexity of these processes, computer modelling is an indispensable additional tool.

One process that can create and sustain a suprathermal electron population in laboratory plasmas is heating with rf waves. In particular, current drive by lower hybrid waves or electron cyclotron waves (ECCD) operates specifically on electrons travelling at substantially suprathermal velocities. Theory has succeeded in explaining many aspects of current drive, but discrepancies remain in its localisation and efficiency. The importance of current drive for current profile manipulation and instability control in a next-step fusion device motivates steady interest in these wave-particle interaction processes and in the properties of the corresponding non-Maxwellian distributions.

### 2. Tools on TCV

The TCV tokamak ( $R=0.88$  cm,  $a=0.25$  cm,  $I_p < 1$  MA,  $B_T < 1.54$  T) is equipped with a 4.5 MW EC heating system. ECCD efficiency in TCV has been generally underestimated by linear theory (by factors ranging from 1.2 to 3) and overestimated by Fokker-Planck quasilinear theory, which predicted strong nonlinear enhancement by the unequalled EC power densities achieved in TCV.

Our main diagnostic tools are a hard X-ray (HXR) pinhole camera (on loan from Tore Supra) and a high field side electron cyclotron emission (ECE) system. HXR bremsstrahlung detection is effected by a linear array of CdTe detectors with an intrinsic resolution of  $\sim 7$  keV [1], which view the plasma vertically along 14 chords that span the outboard half of the cross sec-

tion with a radial resolution of  $\sim 2$  cm on the midplane. Eight energy channels, with adjustable thresholds within the 10-200 keV range, are available for each chord.

The second harmonic X-mode ECE radiometer [2] comprises 24 channels in the 78-114 GHz range, each with a bandwidth of 750 MHz, and observes the plasma along one of two possible horizontal viewlines on the high field side. A third, low field side viewline is also available. The EC radiation observed on the high field side is dominated by relativistically downshifted emission by the higher energy electrons.

Modelling is performed with the CQL3D code, which solves the Fokker-Planck equation in two velocity and one spatial dimensions [3]. The equation includes a quasilinear EC wave damping term, a relativistic collision operator and a model for radial diffusion, with an optional linear dependence on the parallel velocity and a particle-conserving advection term.

### 3. Dynamical observations

It is observed that suprathermal populations are generated when the EC toroidal injection angle  $\phi$  is nonzero, as required for ECCD, whereas in pure heating mode the distribution remains essentially Maxwellian [4]. Figure 1 shows the effect of sweeping  $\phi$  during a plasma discharge ( $n_{e0}=2.5 \times 10^{19} \text{ m}^{-3}$ ,  $\kappa=1.6$ ) on two out of three launchers: while the bulk temperature and the lower energy HXR signal remain constant, the high energy HXR emission and the ECE radiative temperature increase rapidly with  $\phi$ .

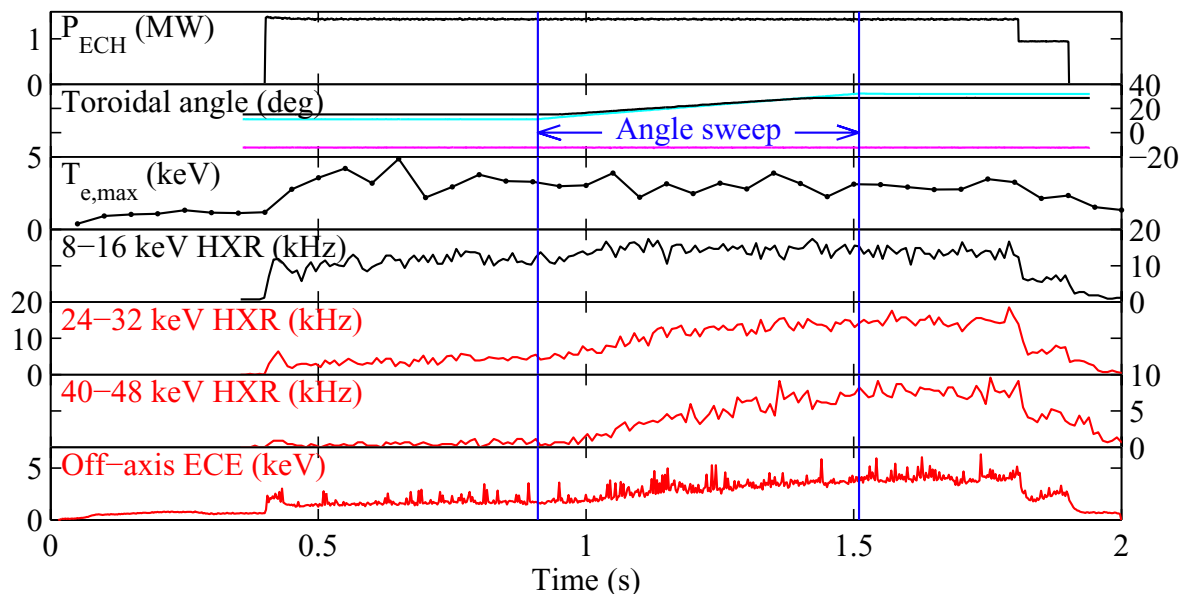


**Fig. 1** Sweep of the EC toroidal injection angle on two out of three launchers: the traces shown are the total EC power, the toroidal angles of the three launchers, the peak electron temperature, three energy channels of the HXR signal on a central chord and an off-axis ECE signal.

The suprathermal dynamics will be dominated by the shortest relaxation time in the system. A fundamental question is whether this is the collisional slowing-down time ( $\tau_{sd}$ ) or a transport time stemming from an anomalous cross-field diffusivity  $D$  ( $\tau_D \sim a^2/D$ ). If  $\tau_{sd}$  is the relevant time scale, the effect of diffusion will be to broaden the fast electron profile by  $\Delta w \sim (D\tau_{sd})^{1/2}$ ; as an example, a diffusivity of the order of the bulk thermal diffusivity,  $D \sim 3 \text{ m}^2/\text{s}$ , would broaden a 120 keV population profile in these plasmas by 11 cm, i.e. one-half the minor radius. It must be noted, however, that  $D$  has been generally estimated to be between

0.3 and 1.0 m<sup>2</sup>/s for the suprathermals sustained by lower hybrid current drive, with the exception of JET (where  $D \sim 6\text{--}10$  m<sup>2</sup>/s) [5].

To study the dynamical evolution at switch-on and switch-off, we have applied square-wave modulation to the EC power and used coherent averaging on the HXR signals to enhance the photon statistics. Photon statistics also rule out a perturbative study, dictating high power levels (2.35 MW) which strongly modulate the target plasma conditions. This causes a major difficulty, as the bulk energy confinement time is of the same order as the slowing-down time for electrons travelling at 5 to 8 times the thermal velocity. Indeed, the bulk temperature rise and fall occur over the same time scales as the HXR and ECE signals. Obviously, keeping the relevant time scales separated will be difficult in any high power current drive studies.

Here, we focus on the time evolution of the HXR *spectrum*. If  $\tau_{sd} \ll \tau_D$ , the spectra must be determined by local properties, with no effective communication over distant regions in space. In particular, since heating is applied to different velocity classes in different spatial regions, because of the Doppler shift needed to match the resonance condition locally, the spectral shape should generally vary in space as well. However, in the relaxed state we invariably find that the spectral shape is essentially constant in space, even well outside the theoretical deposition region (albeit at much lower amplitude) [6]; this is most naturally interpreted as an equilibration resulting from radial diffusion, but could also indicate an anomalous deposition profile in both physical and velocity space.

Stronger evidence for the role of diffusion is provided by the time evolution reconstructed by coherent averaging. As shown in Fig. 2(a) for a case with central co-ECCD ( $\phi=29^\circ$ ), immediately after switch-on the on-axis and far off-axis spectra are very different, the former being larger at low energy and vice versa. As time goes on, the spectral shapes become similar. Figure 2(b) generalises this observation by depicting the profile of the photon “temperature” (from a linear fit to the logarithmic spectra) on the line-integrated signal as a function of the normalised radius: the temperature is initially larger off-axis but evolves over about 10 ms to the familiar constant profile. This effect points clearly to a spatial equilibration: the initially higher off-axis energies are consistent with the larger resonant velocities in that region, while the final relaxed state is everywhere close to the initial temperature on-axis, where most of the power is depos-

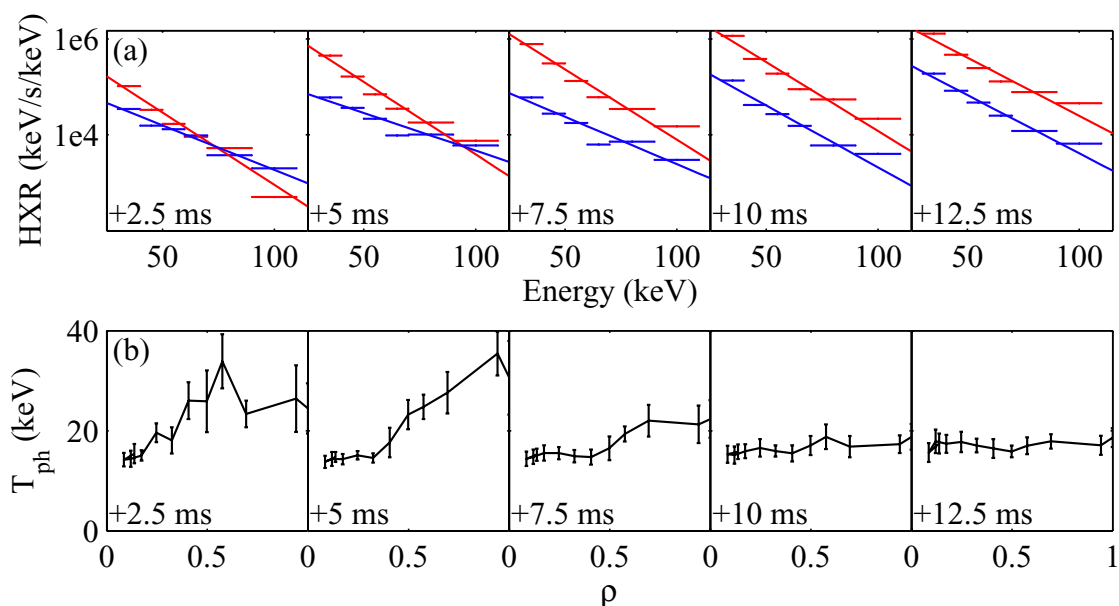


**Fig. 2** (a) HXR emissivity as a function of energy in 5 snapshots after the ECCD switch-on ( $t=0$ ), for a central (red) and an off-axis (blue,  $\rho \sim 0.6$ ) chord; (b) spatial profiles of the photon temperature for the same snapshots ( $\rho$  here indicates the minimum normalised radius for each chord, i.e. the point of tangency to the flux surface).

ited. From the characteristic times observed in these shots, we can set an approximate lower bound  $D > 1.5 \text{ m}^2/\text{s}$ .

#### 4. Fokker-Planck modelling

The discrepancies mentioned at the outset between theory and experiment on the ECCD efficiency have been resolved by including a diffusion coefficient in the Fokker-Planck code. With  $D \sim 3 \text{ m}^2/\text{s}$ , the experimentally measured EC-driven current can generally be reproduced [7].

The CQL3D code can also calculate the HXR emission for direct comparison with the experimental data. Without diffusion, not only is the predicted current much too large, the predicted HXR signal is also far narrower spatially than the measured one. Much better agreement is obtained with  $D = 3 \text{ m}^2/\text{s}$ , as shown in Fig. 3 for a discharge with 0.45 MW central co-ECCD ( $\phi = 16^\circ$ ).

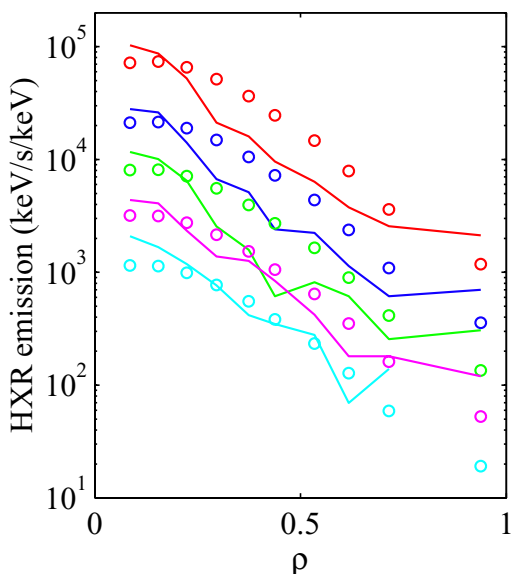


**Fig. 3** (a) Predicted (lines) and measured (circles) HXR emission as a function of chordal spatial location for 5 energy channels of 8 keV width in the 16-56 keV range (descending amplitude for increasing energy).

The absolute amplitude in the centre and the energy dependence are well reproduced, although the spatial profiles are not in complete agreement.

A considerable body of evidence is thus now behind the conclusion that radial transport plays a fundamental role in suprathermal electron dynamics in TCV and in the physics of ECCD. In the future, we plan to extend these studies to a broader parameter range and to exploit the tools described in this paper in a more integrated way, particularly through a calculation of the ECE signals coupled to the Fokker-Planck code.

#### Acknowledgments

The loan of the HXR camera and associated electronics by the CEA is gratefully acknowledged. Thanks are due to the TCV team for the operation of the tokamak and of the auxiliary heating systems. This work was supported in part by the Swiss National Science Foundation.

#### References

- [1] Y. Peysson, S. Coda and F. Imbeaux, Nucl. Instrum. and Methods in Phys. Res. A **458** (2001) 269; Y. Peysson and F. Imbeaux, Rev. Sci. Instrum. **380** (1999) 3987.
- [2] P. Blanchard et al., this conference.
- [3] R.W. Harvey and M.G. McCoy, in Proc. IAEA TCM/Advances in Simulation and Modeling in Thermonuclear Plasmas, Montreal (1992)
- [4] S. Coda et al., Proc. 26th EPS Conf. on Controlled Fusion and Plasma Physics (Maastricht 1999), Europhys. Conf. Abstr. **23J** (1999) 1097.
- [5] Y. Peysson, Plasma Phys. Control. Fusion **35** (1993) B253.
- [6] S. Coda et al., Proc. 28th EPS Conf. on Controlled Fusion and Plasma Physics (Madeira 2001), Europhys. Conf. Abstr. **25A** (2001) 301.
- [7] R.W. Harvey, O. Sauter, R. Prater, and P. Nikkola, Phys. Rev. Lett. **88** (2002) 205001.